Encoding of Temporal Signals by the TGF-β Pathway and Implications for Embryonic Patterning

Benoit Sorre,[1,2,3] Aryeh Warmflash,[1,2,3] Ali H. Brivanlou,[1,*] and Eric D. Siggia[2,*]
[1]Laboratory of Molecular Vertebrate Embryology, The Rockefeller University, New York, NY 10065, USA
[2]Center for Studies in Physics and Biology, The Rockefeller University, New York, NY 10065, USA
[3]Co-first author
*Correspondence: brvnlou@rockefeller.edu (A.H.B.), siggiae@rockefeller.edu (E.D.S.)
http://dx.doi.org/10.1016/j.devcel.2014.05.022

SUMMARY

Genetics and biochemistry have defined the components and wiring of the signaling pathways that pattern the embryo. Among them, the transforming growth factor β (TGF-β) pathway has the potential to behave as a morphogen: in vitro experiments established that it can dictate cell fate in a concentration-dependent manner. How morphogens convey positional information in a developing embryo, when signal levels change with time, is less understood. Using integrated microfluidic cell culture and time-lapse microscopy, we demonstrate here that the speed of ligand presentation has a key and previously unexpected influence on TGF-β signaling outcomes. The response to a TGF-β concentration step is transient and adaptive: slowly increasing the ligand concentration diminishes the response, and well-spaced pulses of ligand combine additively, resulting in greater pathway output than with constant stimulation. Our results suggest that in an embryonic context, the speed of change of ligand concentration is an instructive signal for patterning.

INTRODUCTION

The morphogen model (Wolpert, 2006) posits that during embryonic development, the morphogen level conveys positional information and determines cell fate. This simple picture is complicated by the fact that morphogen levels in a developing tissue are not static (Harvey and Smith, 2009; Kerszberg and Wolpert, 2007; Lee et al., 2001; Schohl and Fagotto, 2002) and that the temporal history of stimulation can have an influence comparable to morphogen levels on patterning (Kutejova et al., 2009). The range of possible dynamic signals that could be encountered during development is quite diverse: a monotone increasing signal patterns the vertebrate dorsoventral axis (Schohl and Fagotto, 2002), the fly wing disc (Wartlick et al., 2011), and the neural tube (Balaskas et al., 2012); oscillatory signals occur during somatogenesis (Aulehla and Pourquié, 2010); and pulsatile signals were recently observed in *Xenopus* animal caps (Warmflash et al., 2012). However, because the dynamics of the ligands that initiate these events in a developing embryo are often hard to discern and to manipulate, it is difficult to disentangle the relative contributions of morphogen levels and dynamics of ligand presentation to the downstream response.

Here we examine how the time course of ligand presentation affects the activity of transforming growth factor β (TGF-β) signaling in the myoblast progenitor C2C12 cell line, a model for TGF-β-regulated signaling and differentiation (De Angelis et al., 1998; Katagiri et al., 1994; Liu et al., 2001). We adapted an automated microfluidic cell culture platform (Gómez-Sjöberg et al., 2007) that allows us to apply complex time courses of stimulation and record individual cell responses in real time with video microscopy (Figure S1 available online). Cells grew in the microfluidic chambers at a rate comparable to that observed in regular cell culture dish, and growth was unaffected by either imaging or TGF-β1 stimulation (Figure S2). This approach allows a direct and quantitative measurement of the relationship between the dynamics of ligand presentation, transcriptional response, and the specification of discrete fates.

The transcriptional response to TGF-β signaling is mediated by the complex of a receptor-activated Smad (R-Smad) with the coregulator Smad4. Ligand binding to TGF-β receptors leads to R-Smad phosphorylation, complex formation with Smad4, and nuclear translocation (Massagué et al., 2005). Receptor Smad2 and Smad3 respond specifically to activin, nodal, and TGF-β ligands, whereas receptor Smad1, Smad5, and Smad8 respond to bone morphogenetic proteins (BMPs) and growth and differentiation factors (Figure 1A). Using cells expressing a GFP-Smad4 fusion, we have recently shown that the response to a step increase in TGF-β1 was transient and adaptive: even though the R-Smad, Smad2, and Smad3 remained phosphorylated and localized to the nucleus for as long as TGF-β ligand was present in solution, transcription, measured either by RT-PCR of endogenous target genes or synthetic TGF-β reporters, terminated after about 4 hr (Warmflash et al., 2012) (Figures 1B–1H and S2N–2P). The C2C12 cell lines stably transfected with fluorescently labeled Smads as reporters responded normally to stimulation compared to untransfected cells, and the temporal profile of GFP-Smad4 nuclear localization tracked transcriptional activity of endogenous target genes under all conditions examined (Warmflash et al., 2012). The fluorescent Smad4 fusion protein is therefore an attractive reporter of pathway activity since it reveals the immediate consequences
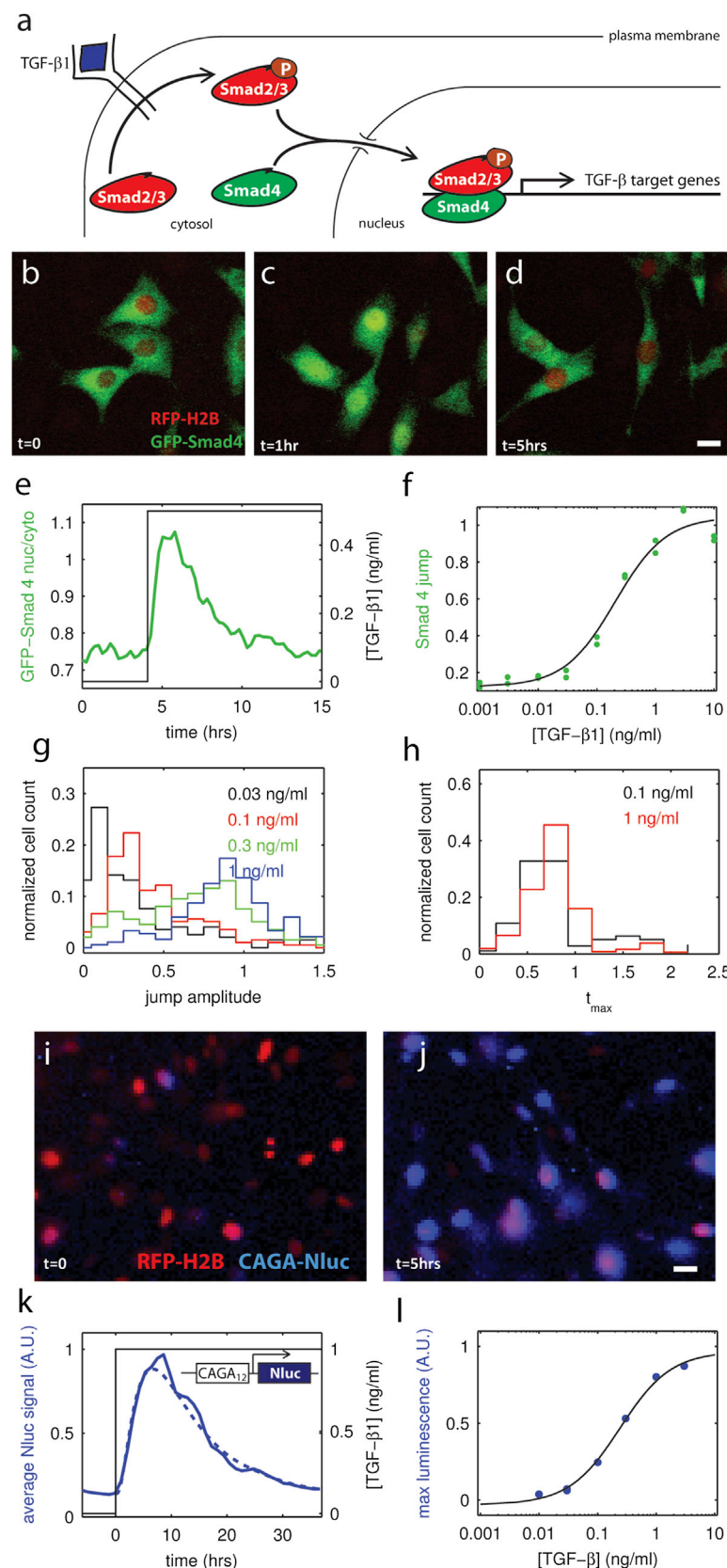
Figure 1. Pathway Response to a Ligand Step Is Adaptive and Graded

(A) Components of the TGF-β signal transduction cascade.

(B–D) Evolution of GFP-Smad4 (green) intracellular localization after a step stimulation with TGF-β1. Before stimulation GFP-Smad4 is mostly cytoplasmic (B); GFP-Smad4 is relocalized in the nucleus 1 hr after the start of stimulation (C) and returns to the cytoplasm by t = 5 hr (D). Scale bar, 20 μm.

(E) Average nuclear to cytoplasmic ratio of GFP-Smad4 as a function of time in response to a step increase of TGF-β1 concentration from 0 to 0.5 ng/ml (n ∼ 400 cells).

(F) Dose-response curve for GFP-Smad4. The "Smad4 jump" response is defined as the maximum in the Smad4 curve relative to the prestimulus baseline (see Figure S1D). Each point is the average of the jumps of all the cells present in one chamber (n ∼ 400). Data from two different chambers are plotted. The response (I) is well fit by the expression $I = a \times (L/K + L) + b$, where L is the ligand concentration, $K = 0.20 \pm 0.08$ ng/ml is the inflection point, and a and b are two constants (black line).

(G and H) Statistical analysis of single-cell response for a few TGF-β1 concentrations. The distribution of single-cell response amplitude ("jump") is single peaked and graded with ligand level (G). Most cells respond within 1 hr of the step up in ligand irrespective of ligand level (H).

(I and J) Evolution of NLuc signal in single cells after a step stimulation with TGF-β1. Around 5 hr after of beginning of stimulation, an 8- to 10-fold increase of the luminescence signal (blue) is observed. NLuc was fused to a nuclear localization signal (NLS) to simplify image analysis. Scale bar, 20 μm.

(K) Average transcriptional activity downstream of TGF-β stimulation (n ∼ 400), as measured by the luminescence signal of the CAGA$_{12}$-NLuc reporter, as a function of time in response to a step increase of TGF-β1 concentration. Dotted line: fit of our adaptive model (see Supplemental Experimental Procedures, section 6).

(L) Dose response of TGF-β-induced luminescence signal of the CAGA$_{12}$-NLuc reporter. The response is defined as the maximum in the average luminescence curve relative to the prestimulus baseline, normalized by the response to the highest dose (n ∼ 400). The response (I) is well fit by the expression $I = a \times (L/K + L) + b$, where L is the ligand concentration, $K = 0.24 \pm 0.1$ ng/ml is the inflection point, and a and b are two constants (black line).

See also Figures S1 and S2.

of receptor activation, and when coexpressed with a nuclear marker, is very amenable to quantitative single-cell imaging.

However, in order to understand how pathway activity is interpreted at the level of gene expression, the dynamics of Smad transcription factors should be correlated to the downstream transcriptional response. Traditional population assays destroy the sample, assume homogeneity, and could not practically follow the complex stimuli we apply; we wanted instead to be able to measure transcriptional response in real time and with single-cell resolution. For that purpose, we fused a synthetic promoter (Dennler et al., 1998) specific to the Smad3 branch of the TGF-β pathway (CAGA$_{12}$) to the NanoLuc luciferase (NLuc), an engineered luminescent protein (Hall et al., 2012) that is more than 100× brighter than its *Firefly* and *Renilla* variants and therefore allows for detection of luminescence in single cells (Figure S1). An identical construct with the NLuc replaced with GFP yielded fluorescence below background levels in our cells. Luminescence does not suffer from autofluorescence or excitation backgrounds, and it allows for longer exposure times and therefore greater sensitivity. A synthetic reporter eliminates potential transcriptional feedback that could modulate a natural promoter. Since the substrate for NLuc was unstable under cell culture conditions, time-lapse imaging required our microfluidic technology to apply fresh substrate each time an image was acquired and wash it off afterward, minimizing toxicity. Periodic exposure to substrate also conveniently destabilized NLuc, thus lowering background and revealing the transcriptional response with better temporal resolution. The CAGA$_{12}$-NLuc-induced luminescence could readily be observed using a standard microscopy charge-coupled device camera with 2 min exposure time, and addition of TGF-β1 ligand triggered an 8- to 10-fold increase of the signal (Figures 1I–1L). See Experimental Procedures, Supplemental Information, and Figure S1 for a complete characterization of our CAGA$_{12}$-NLuc reporter system.

RESULTS

TGF-β Pathway Response Is Adaptive and Graded

To establish how C2C12 cells encode different levels of morphogen and to make sure cells behaved the same way in the microfluidic chip as in a regular cell culture dish, we first asked how cells respond to a step increase in TGF-β1 ligand for various concentrations (Figures 1B–1F). These time courses of stimulation provide a dose-response calibration and serve as a reference for the more complex temporal stimulations examined below. Culture medium containing different concentrations of TGF-β1 ligand was renewed every hour to ensure proper control over the ligand concentration. Comparison of the dose response with prior experiments in regular cell culture conditions rules out significant ligand depletion at low concentrations in the small microfluidic chambers. Consistent with our previous experiments (Warmflash et al., 2012), GFP-Smad4 only localized transiently to the nucleus following the step, despite continuous stimulation (Movie S1). Single-cell analysis showed that for all concentrations, the vast majority of cells responded in a graded manner to the ligand step, with a pulse that peaks within 1 hr (Figures 1G and 1H and S2). We observed that full GFP-Smad4 adaptation depends on cell density (Figure S2Q). In the following, to ensure consistency between experiments, we worked in conditions

where adaption was complete (initial density, ∼300 cells/chamber). The transcriptional response measured with our CAGA$_{12}$-NLuc reporter is also transient (Figure 1K).

We used modeling to show that all the time-dependent stimuli assayed by NLuc expression were consistent with a simple phenomenological model. Unlike previous modeling work focusing on the molecular details of the pathway (reviewed in Zi et al. [2012]), our model defines the response with only two rate parameters, a timescale for adaptation and the ∼5 hr NLuc half-life (Figure 1K). See also the Experimental Procedures and Supplemental Experimental Procedures, section 6, for a complete description of the fitting procedure. The best fit required TGF-β-driven transcription to be adaptive, with a peak about 1 hr after a step in ligand stimulation. This agrees with the observed dynamics of GFP-Smad4 and is a further consistency check. Finally, as with GFP-Smad4, the NLuc dose response is graded with concentration and follows a simple sigmoidal curve (Figure 1L).

Pulsed Stimulation Increases Pathway Throughput

We have previously shown that Smad4 pulses repetitively into the nucleus in blastula- and gastrula-staged *Xenopus* animal caps (Warmflash et al., 2012). To investigate the consequences of pulsing, we stimulated cells with 1 hr pulses of TGF-β1 separated by 6 hr and obtained a transient response for each pulse (Figure 2A; Movie S2). Under the same stimulation protocol, the signal from the CAGA$_{12}$-NLuc reporter approximately doubles from the first pulse to the second and then saturates at a value representing the balance between its production and decay that was fit with the same model and parameters as for the step stimulation (Figure 2B) and mathematical supplement. If the protein was stable, its accumulation would simply count the number of pulses. At the single-cell level, there is no correlation in the amplitude of response to successive pulses repeated every 6 hr (Figure S3), and pulses of different heights elicit an autonomous response independent of the previous pulse (Figure 2D). When the pulse repeat rate becomes comparable to the adaptation time, there is a diminished response around an elevated plateau (Figures 2C and S3A–S3L). The single-cell responses are reduced in amplitude but still uncorrelated from pulse to pulse (Figure S3). For an adaptive system, such as the system described in Figure 1, pulsatile stimulation could be a mechanism for overcoming adaptation to continuous simulation and increasing pathway throughput.

C2C12 Differentiation Is Blocked More Effectively by TGF-β Pulses Than Continuous Stimulation

We next addressed the consequences of pulsed ligand delivery for cell fate specification. The C2C12 progenitors can differentiate to myotubes when exposed to differentiation medium (DM), and presentation of TGF-β1 inhibits this differentiation (Figure 2E). Working in a standard cell culture dish, we compared the ability TGF-β1 to block cell differentiation when presented either continuously during 15 hr or as three 1-hr-long pulses separated by 6 hr, spanning the same total time (Figure 2F). We controlled for TGF-β1 lifetime by using the same TGF-β1-containing media to create the three pulses. After 24 hr, we used immunofluorescence to quantify the fraction of cells expressing myogenin, an early marker of commitment to terminal myotube differentiation (Tapscott, 2005) (Figures 2E–2K and S3M–S3T). Again, pulsatile stimulation proved to be more effective at blocking differentiation, and
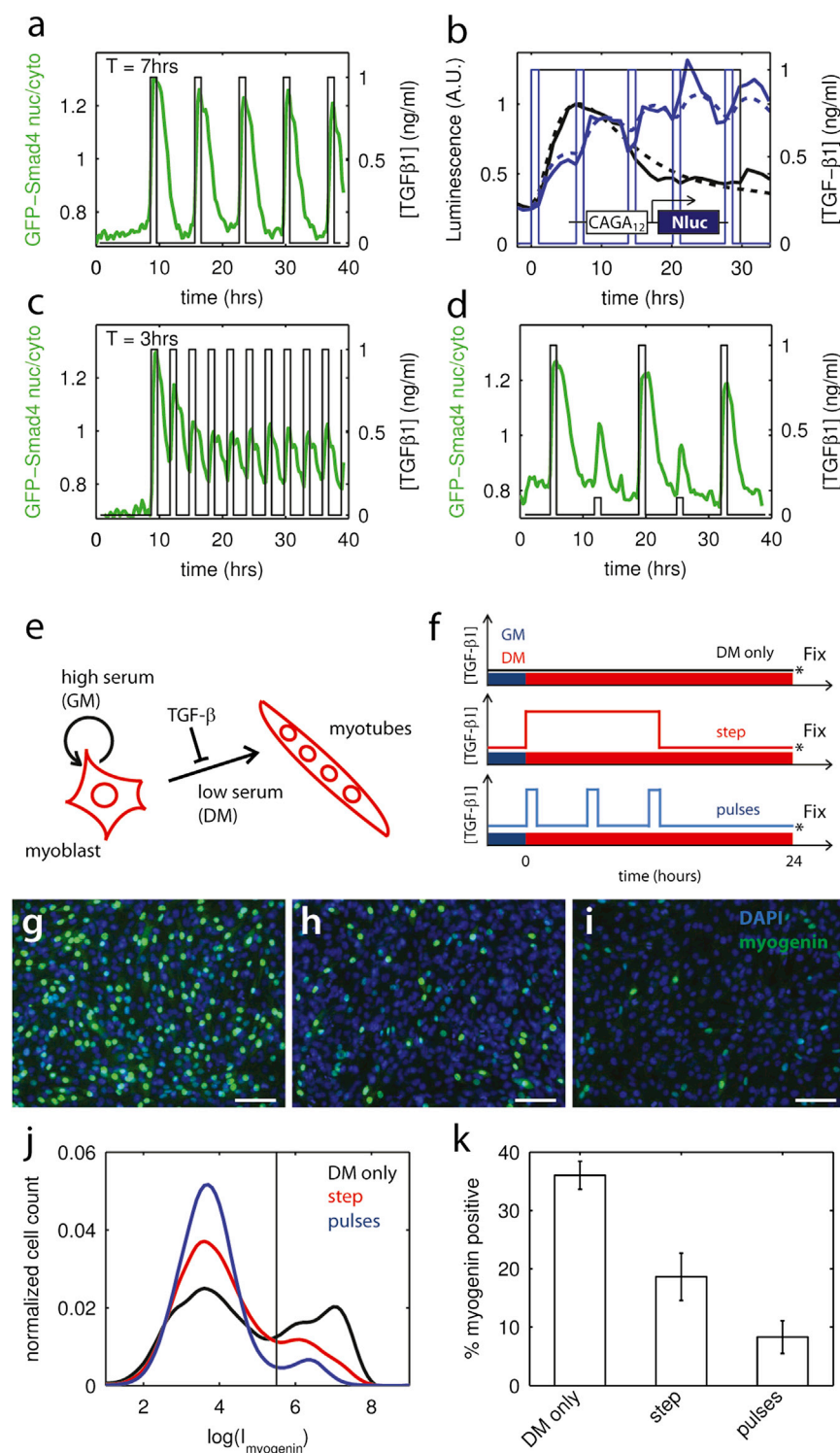
Figure 2. Pulsed Stimulation Increases Pathway Throughput and Fate Regulation

(A) Evolution of GFP-Smad4 nuclear to cytoplasmic ratio (thick line, left axis) in response to a pulsatile stimulation. Period of stimulation is 7 hr.

(B) Comparison of the transcriptional activity downstream of TGF-β stimulation, as measured by the luminescence signal of the $CAGA_{12}$-NLuc reporter, when the cells are stimulated with a step (black) or pulsed (blue) stimulation. Dotted lines: fit using the same model parameters as in Figure 1K.

(C) Same as in (A), but with a period of stimulation of 3 hr, showing that when the frequency of stimulation is increased, the amplitude of the averaged response to each pulses decreases.

(D) Same as in (A), but with pulses of variable amplitude, showing no memory in the response.

(E) Differentiation program of the myoblastic cell line C2C12. GM, growth medium.

(F) Experimental procedure: exposure to DM alone is contrasted with continuous 15 hr exposure or three 1 hr pulses of TGF-β1. The concentration was 0.1 ng/ml in all cases.

(G–I) Immunofluorescence staining of the cultures against myogenin (green channel). (G) Control DM only. (H) DM + TGF-β1 step. (I) DM + TGF-β1 pulses. Counterstain, DAPI (blue). Scale bar, 100 μm.

(J) Normalized distribution of single-cell intensity of myogenin signal for the three conditions color coded as in (F). Cells can be separated in two populations: myogenin negative or myogenin positive based on fluorescent intensity. For each condition, n > 10,000. Vertical line represents the threshold between the two populations.

(K) Comparison of the percentage of myogenin-positive cells, as defined in (F), for the three conditions. The pulses are on average 2.5 times more effective that the step in preventing differentiation ($p < 10^{-5}$). Error bar are given by the SEM from ten randomly selected fields.

See also Figure S3.

portional to the number of pulses (2.5 times from three pulses). Pulsed stimulation is a general mechanism to bypass internal feedbacks limiting pathway output. This mechanism could be at work in blastula- and gastrula-staged *Xenopus* animal caps, where all timescales are shorter (Warmflash et al., 2012).

Pathway Activity Depends on the Speed of Concentration Increase

Another generic property of adaptive systems is that their response depends not

2.5 times fewer cells expressed myogenin in the pulsatile case (p value $< 10^{-5}$ versus step simulation), despite the fact that the total duration of ligand exposure was only 3 hr compared to 15 hr in the step stimulation. Thus pulsed stimulation with a period exceeding the adaptation time enhances both total transcriptional activity and the regulation of cell fate, and the effect is nearly proportional

only on the level but also on the rate of stimulation (Tu et al., 2008). Adaptation to a step in stimulus suggests that the system filters out the concentration of ligands that change slowly in time irrespective of their absolute level. To probe this aspect of the temporal response of the pathway, we stimulated the cells with a linear ramp in ligand at various rates of increase (Figures
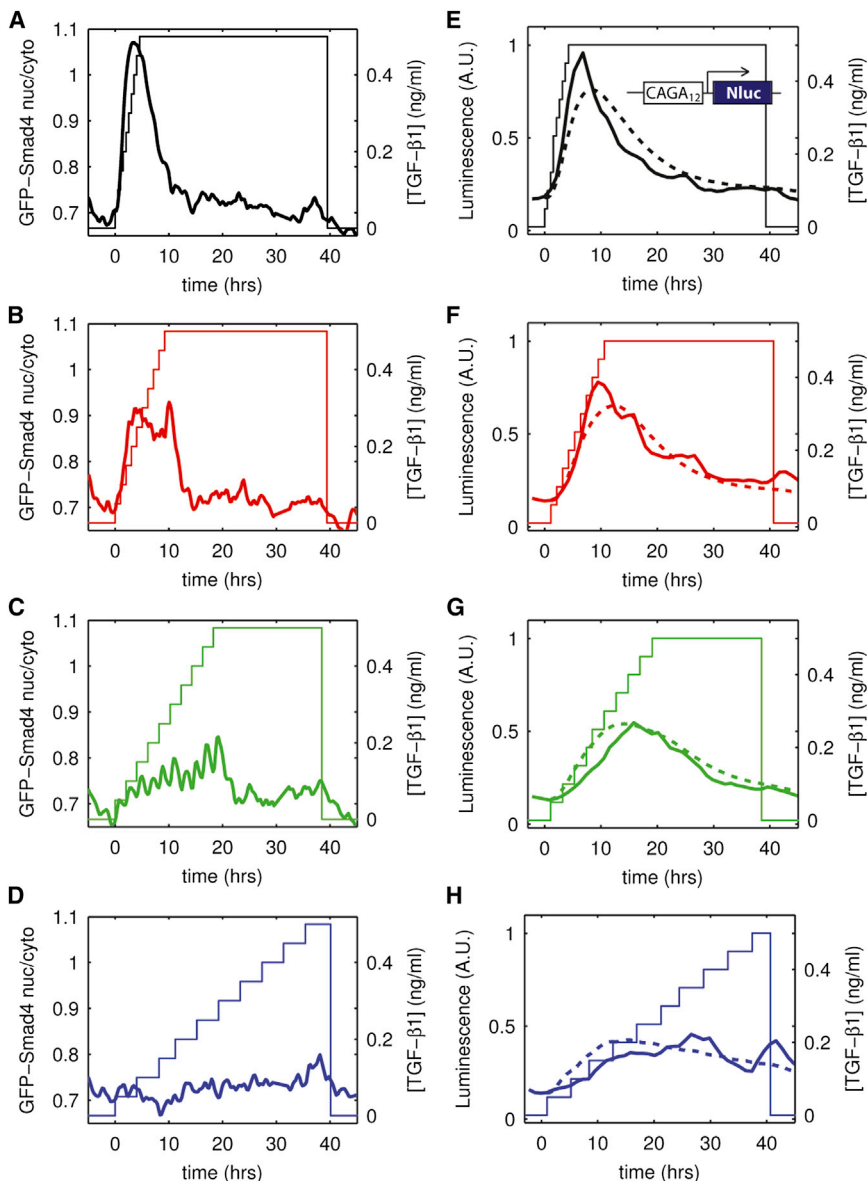
Figure 3. Pathway Activity Depends on Rate of Change

(A–D) Evolution of GFP-Smad4 nuclear to cytoplasmic ratio (thick lines, left axis) in response to increases of the TGF-β1 concentration (right axis) from 0 to 0.5 ng/ml (a nearly saturating dose) at various rates of increase.

(E–H) Evolution of the transcriptional activity downstream of TGF-β stimulation, as measured by the luminescence signal of the CAGA$_{12}$-NLuc reporter in response to increases of the TGF-β1 concentration from 0 to 0.5 ng/ml (a nearly saturating dose) at various rates of increase. Dotted lines: fit using the same model parameters as in Figure 1K.

pathway can learn its position relative to a source. Consider a morphogen that diffuses from a source and is degraded. Its steady-state profile is exponential (Figure 4A), but the speed of morphogen increase also depends on the distance to the source (Figure 4B). We can now contrast how two pathways, a "linear" and an "adaptive" pathway, will respond to this ligand time course and extract positional information. The linear pathway responds only to ligand level (Figure 4C), while the adaptive pathway is sensitive to both level and speed, and its response to a step is transient (Figure 4D). Both pathways will produce a response that depends on the distance to the source (Figures 4E and 4F); however, the fact that the adaptive response peaks well before the linear response reaches steady state would tend to suggest that the time required for a fate decision is much less for cells using an adaptive pathway. This could well confer a fitness advantage in rapidly developing embryos (Figures 4G and 4H). To test that idea, we

3A–3D). We found that when the increase is sufficiently fast compared to the adaptation time, the response was comparable to step stimulation. The maximum in the GFP-Smad4 response curve clearly decreased with decreasing ramp rate (Figures 3A–3D). The single-cell response became more diffuse in slow ramps in comparison to steps (Figure S4A), as expected for an adaptive system. Again, the transcriptional response measured with the CAGA$_{12}$-NLuc is consistent with the observation made with GFP-Smad4, as confirmed by the fits (Figures 3E–3H, S4, and Supplemental Experimental Procedures, section 6). The rate of ligand delivery has a pronounced effect on cellular response to TGF-β stimulation: the response to a given level can be all or nothing depending on the speed at which the concentration has been increased.

Our observation that the speed of increase of concentration is as relevant as concentration itself has important consequences as to how a cell reading the morphogen through an adaptive

have utilized the pathway responses from Figures 4E and 4F as the input to a gene regulatory network (GRN) (Saka and Smith, 2007) featuring the minimal set of elements to achieve fate determination: mutual repression between fates and bistability (see Figure 4G and Supplemental Experimental Procedures, section 7). Factor B is more sensitive to TGF-β and is excluded from the region of highest morphogen by repression from factor A. The GRN responds rapidly so as to track the pathway response, and the bistability then locks in the maximum signal seen by a cell. We chose the parameters of the GRN for each case so that the adaptive and linear models resulted in identical spatial patterns and then compared the time to achieve those patterns. The result is clear-cut: the final French flag pattern is reached three times faster if an adaptive pathway is used to read the morphogen gradient (Figures 4H and 4I and Movie S3).

The dynamic response of the adaptive pathway also has the advantage that it is insensitive to ligand dynamics: a 10-fold
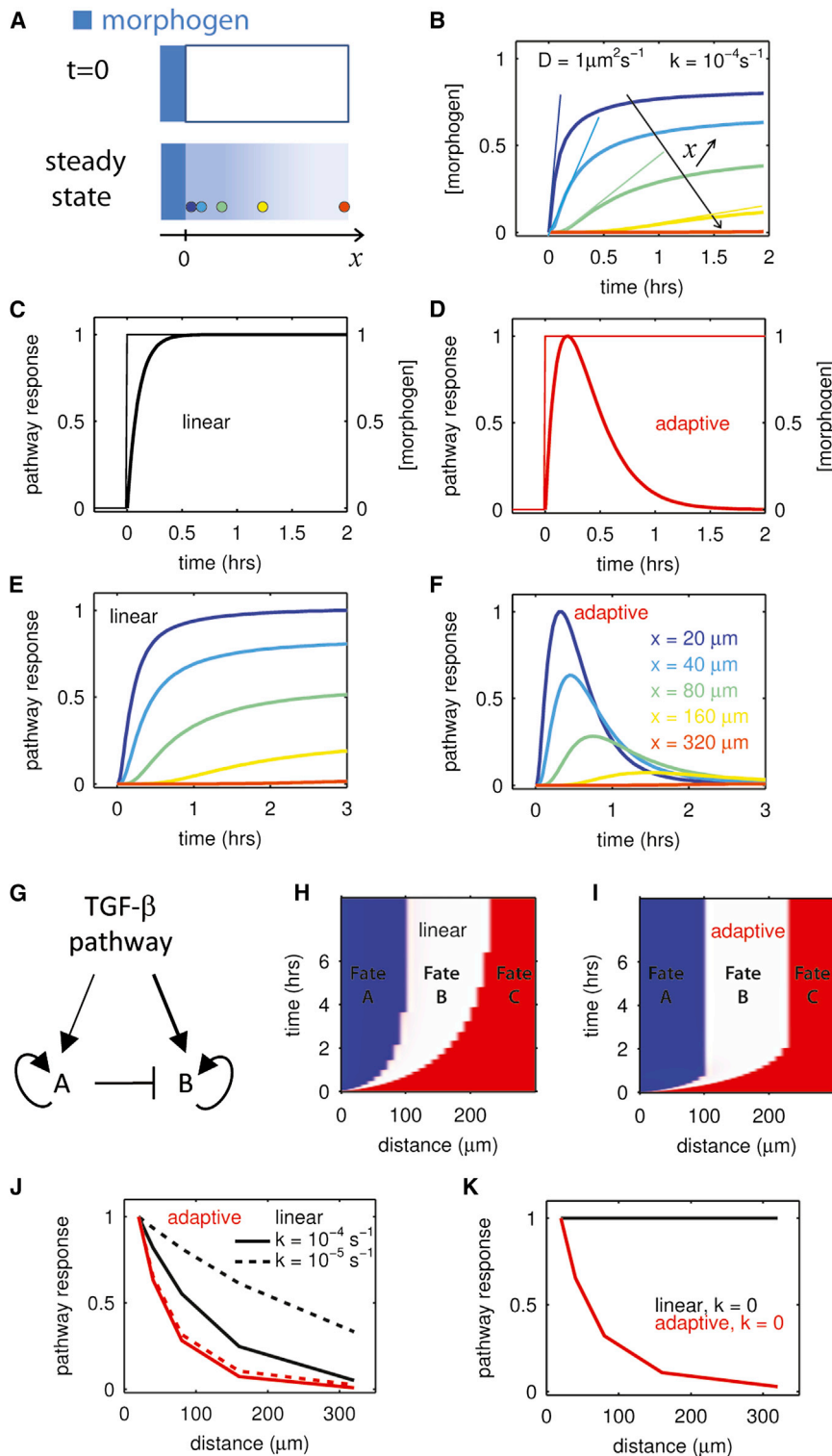
Figure 4. Speed Fating: An Adaptive Signaling Pathway Can Extract Positional Information without a Spatial Gradient

(A) At t = 0, a morphogen (in blue) is allowed to diffuse in a tissue from a constant source located in x = 0 (upper panel). The diffusion constant is D and ligand decays at a rate k. In such conditions, the steady state profile of concentration is an exponential gradient with characteristic length $\lambda = \sqrt{D/k}$ (lower panel). Colored circles represent cells at various distances from the source.

(B) The temporal profile of ligand concentration, calculated at various distances from the source (x) and for ligand parameters, D, k, characteristic for embryonic development (Müller et al., 2012), show that both the steady-state concentration and the speed at which this steady state is reached depend on the distance to the source. Color code in (A) or (F).

(C and D) Comparison of a linear pathway (C) and an adaptive pathway (D) responding to a ligand step as in (B);. For the "linear" pathway, the response (y) to ligand input (I) is given by the differential equation $\dot{y} = I - cy$, where c sets the time scale of response. The adaptive pathway is defined by the system $\dot{y} = I - cy - 0.25c^2.x; \dot{x} = y$ (see Supplemental Information) where again c sets the response time and x is a feedback. The reaction time of both pathways is defined to be identical ($c = 10h^{-1}$), and both of them have an amplitude of response that is linear with the ligand concentration. As a consequence they would show an identical dose-response curve to ligand presented as a step.

(E) Response of the linear pathway (C) to the different ligand profiles presented in (B). The linear pathway can extract positional information, i.e., the observed response varies as a function of the distance from the morphogen source. Color code for distance follows (F).

(F) Response of the adaptive pathway (D) to the different ligand profiles presented in (B) depends on the distance to the morphogen source. However, the differentiation decision, defined by the time of the response maximum in the adaptive case or when the response saturates for the linear pathway, can be faster in the adaptive system.

(G) Minimal GRN for fate decision between two fates (A and B) induced downstream of TGF-β pathway activity. Factor A is activated at lower TGF-β levels than factor B, as depicted by the thickness of the arrows.

(H and I) Establishment of a French flag pattern in function of time for a linear (H) or adaptive (I) pathway. Fate A (blue) and fate B (white) are induced downstream of TGF-β signaling, and A represses B as in the GRN described in (G). Fate C (red) represents the default fate (both A and B are off). When an adaptive pathway is used, the final pattern is reach three times faster.

(J) Comparison of how the two pathways extract positional information from a spreading gradient of morphogen. The adaptive pathway is more efficient at patterning since its distance-response curve is much sharper. Furthermore, the response-distance function of the adaptive system is insensitive to changes in morphogen properties (dotted lines, 10-fold decrease in decay rate), whereas the linear pathway is sensitive.

(K) In the extreme case of no ligand decay ($k = 0$), the steady-state concentration profile does not depend on position, but the adaptive pathway can still extract position information, while the linear pathway fails to do so.

See also Figure S4.

decrease in the ligand decay rate leaves the relative response as a function of distance unchanged for the adaptive pathway, while it becomes much flatter for cells using a linear pathway (Figure 4J). Nothing changes with the adaptive pathway in the extreme case that the morphogen does not decay at all, while the linear pathway conveys no information about position in this condition (Figures 4K and S4I and S4J. We term positional information acquired through an adaptive pathway "speed fating."

DISCUSSION

The influence of the speed of increase of morphogen concentration on cell response has been generally overlooked. This is mostly because the key experiments (Green et al., 1992; Gurdon et al., 1999), including our own (Wilson et al., 1997), that established that both the activin/nodal and BMP branches of the TGF-β pathway behave as morphogens, i.e., that different concentrations of ligand could give rise to different fates, were performed by delivering ligand steps or short pulses of variable height to isolated *Xenopus* blastula cells, in vitro. More realistic temporal stimuli were not considered. In particular a ligand step does not discriminate between an adaptive response and a response that registers level only.

Static and dynamic positional information are not mutually exclusive, and one biochemical pathway can display either behavior or a blend, depending on kinetic parameters. Their relative contribution can drift during evolution, while the complex downstream transcriptional gene network that assigns distinct fates to pathway output remains invariant (Balaskas et al., 2012; Saka and Smith, 2007). However the adaptive sensing of position is invariably faster, less contingent on ligand parameters such as decay rate, and inherently more robust to slow changes in protein levels or the environment. Bacterial chemotaxis is a good example of this strategy, and a phenotypic model similar to ours was used to fit ramp stimuli (Tu et al., 2008). Exact adaptation is not required for speed fating, merely maximal response proportional to the time rate of change.

In our experiments the ligand directly activated the pathway, while in the embryo signaling results from a complex interaction of activators and inhibitors. Nevertheless measurement of Wnt, TGF-β, and BMP signaling in *Xenopus* (Lee et al., 2001; Schohl and Fagotto, 2002) shows that activation of the associated transcriptional effectors (β-catenin, Smad2, Smad1) increases in time and does so most rapidly in regions associated with the greatest pathway activity (e.g., ventral for BMP4). What matters for speed fating is the temporal profile of pathway activity, which will obviously integrate contributions of both inhibitors and activators.

Negative feedback following stimulation, either intracellular through receptor inactivation or extracellular through secreted inhibitors, is a very common feature of the signal transduction pathways that are used throughout development and would tend to lead to partial adaptation. So, independently of the exact molecular details that are specific to each system, the possibility that the time derivative of a signal confers positional information has to be considered, and dynamic characterization of signaling pathways in terms of input-output should be included in modern morphogen models.

EXPERIMENTAL PROCEDURES

Microfluidic Cell Culture and Imaging

Cell culture chips were obtained from the Stanford Foundry and controlled by custom-made MATLAB interface adapted from the one kindly provided by the Quake laboratory. Prior to C2C12 cell seeding, chambers were coated with 20 μg/ml fibronectin from bovine plasma (Sigma) for at least 2 hr. The day preceding the experiment, ~100 cells/chamber were seeded. Cells were fed every hour either with growth medium (GM) (Dulbecco's modified Eagle's medium [DMEM] + 10% fetal bovine serum) alone or with GM containing TGF-β1 according to the time course of ligand concentration shown in figures, except for the experiment shown in Figure 3A wherein medium was changed every 0.5 hr. Fluorescence imaging of GFP-Smad4 was performed every 15 min. NLuc luminescence was acquired every hour, and fresh NLuc substrate was provided before each acquisition. Single-cell data were extracted using custom-made MATLAB image analysis routines.

C2C12 Differentiation

At confluence (t = 0), culture medium was switched from GM to either differentiation medium ([DM], DMEM + 2% horse serum) only or DM complemented with 0.1 ng/ml TGF-β1. TGF-β1 was presented either continuously for 15 hr (step) or as three 1-hr-long pulses each separated by 6 hr. To control for ligand consumption/degradation, the medium used for the first pulse was saved and used for the subsequent pulses. All samples were fixed and stained for myogenin (Developmental Studies Hybridoma Bank clone F5D, 1:200) at t = 24 hr, following standard immunofluorescence protocols, as detailed in Supplemental Experimental Procedures.

CAGA₁₂-NLuc Single-Cell Imaging

TGF-β-responsive elements are appealing candidates for a single-cell TGF-β reporter system, but unfortunately they did not produce enough signal for detection at the single-cell level when driving expression of either GFP or firefly luciferase.

We thus switched to NLuc, a small (19.1 kDa) engineered luciferase commercially available from Promega (Hall et al., 2012). The enzyme is advertised to be 150-fold brighter than other luciferases. It uses furimazine, a coelenterazine analog as a substrate. Unfortunately, furimazine is not stable under conventional cell culture conditions (half-life, ~1 hr). In order to solve that issue, we took advantage of the cell culture chip capabilities: the NLuc substrate was kept in a refrigerated container in an oxygen-free atmosphere to prevent its degradation for days. Before each acquisition, fresh substrate (10 μM in DMEM) was flushed over the cells and then rinsed once the picture was acquired, thus minimizing cell exposure to the substrate. We observed that this procedure conveniently destabilized NLuc to about half its half-life (~5 hr). Single-cell luminescence signal was measured once per hour. CAGA₁₂-NLuc luminescence could readily be detected in single cells with 2 min exposure times (objective, 10× 0.45 NA; camera, Hamamatsu ORCA R2, maximum gain, binning 4). See Supplemental Experimental Procedures, section 5, and Figure S1 for a detailed description of the validation of the CAGA₁₂-NLuc reporter system.

Fitting NLuc Transcriptional Response

In order to quantify the degree of internal consistency among our two reporters, GFP-Smad4 and CAGA12-NLuc, for various dynamic stimuli, we have designed a model with only three essential parameters (after allowing for a scale factor to define microscope camera units), each of which can be tied fairly tightly to a single experiment: the timescale of adaptation $(2/c)$, the half maximal effective concentration of the dose-response curve to TGF-β stimulation (K_I), and the lifetime of NLuc (τ). At the core of our signal transduction cascade is an adaptive module. See Figure S4B for a graphic presentation of the model. A linear model for adaptation had the fewest free parameters and proved adequate for our data:

$$\dot{x} = y \qquad \text{(Equation 1)}$$

$$\dot{y} = -\frac{c^2}{4}x - cy + I, \qquad \text{(Equation 2)}$$

where I is the ligand-dependent input and y is the output of the adaptive module. The response of this module following an input step at $t = 0$ is

$$y = Ite^{-ct/2}, \qquad \text{(Equation 3)}$$

which is in good agreement with the single-cell GFP-Smad4 data, in particular because the timescale for adaptation ($2/c$) is ligand independent (Figure 1H) as assumed in the model. It is worth noting that this is not the case with other commonly used adaptive circuits, such as the incoherent feedforward loop where the adaptation time varies with the inverse input level, i.e., I has units of frequency.

Upstream of the adaptive module is a receptor module. The dependence of both Smad4 and NLuc in response to a ligand step L scales as $L/(K_I + L)$ (Figure 1), so it is plausible to simply model the receptor module and its connection to adaptation by

$$I = L/(K_I + L). \qquad \text{(Equation 4)}$$

For the transcriptional output downstream of the adaptive module, we used

$$\dot{z}_1 = \max(0, y) - z_1/\tau \qquad \text{(Equation 5)}$$

$$\dot{z}_2 = z_1 - z_2/\tau, \qquad \text{(Equation 6)}$$

where z_1 can loosely be thought of as message and z_2 as protein (NLuc). The relaxation time τ need not be the same in the two equations, but since the data require $\tau \sim 5$ hr, while the adaptive system has a timescale of ~1 hr, the time course of z_2 is largely insensitive to how relaxation time is distributed between the two equations, so we made the rates equal, thereby eliminating a parameter that would be impossible to fit. Fits of the NLuc data are presented in Figures 1K, 2B, 3E–3H, and S4. A detailed description of the fitting procedure and hypothesis is given in Supplemental Experimental Procedures, section 6.

Model for Dynamic Embryonic Patterning

To reinforce the intuition that adaptive systems can infer position from the rate the ligand changes in time, we consider that argument in a more mathematical manner. As an idealized model of morphogen spreading in an embryo, we consider a ligand (L) that diffuses into the region at $x > 0$, with a diffusion constant (D) from an infinite source in $x = 0$ and that is degraded at a rate (k)

$$\partial_t L(x, t) = D\partial_x^2 L(x, t) - kL(x, t), \qquad \text{(Equation 7)}$$

which gives

$$L(x, t) = \frac{x}{2\sqrt{\pi D}} \int_0^t s^{-\frac{3}{2}} e^{-ks - \frac{x^2}{4Ds}} ds. \qquad \text{(Equation 8)}$$

For $t = \infty$, Equation 8 becomes $L(x) = e^{-\sqrt{k/D}x}$, the exponential gradient of morphogen. We have plotted in Figure 4B the temporal profile of ligand concentrations experienced by cells at various distances from the source of morphogen.

We then compare how a linear pathway and an adaptive pathway respond to the ligand profiles calculated from Equation 8. For the "linear" pathway, the response (y) to ligand input (I) is given by the differential equation

$$\dot{y} = I - cy, \qquad \text{(Equation 9)}$$

where c sets the timescale of response. The adaptive pathway is defined by the system

$$\dot{y} = I - cy - \frac{c^2}{4}x \; ; \; \dot{x} = y, \qquad \text{(Equation 10)}$$

where again c sets the response time and x is a feedback (note this is the same system as the system we used to fit the NLuc data). The reaction time of both pathways is defined to be identical ($c = 10h^{-1}$), and both of them have an amplitude of response that is linear with the ligand concentration. As a consequence they would show an identical dose-response curve to ligand presented as a step (Figures 4E and 4F).

Finally, to make the point that the transcriptional output from adaptive system can reach its maximal value and thus infer position well before the ligand reaches its asymptotic value, we have modeled a bistable GRN that captures the output ($y(t)$) of the signaling pathway from Equation 9 or Equation 10 and renders it permanent. This is very consistent with standard embryology, where a signal is applied during a window of competency, at the end of which the fate of the targets is specified and no longer requires the signal.

A minimal model requires two proteins, A, B, both bistable. They define three territories in order of decreasing signal level: A ON B OFF (blue stripe in Figures 4H and 4I), A OFF B ON (white stripe in Figures 4H and 4I), and both OFF (red stripe in Figures 4H and 4I). This GRN is defined by the arrow diagram in Figure 4G or by the system of equations

$$\dot{A} = m(t) + \frac{A^2}{1 + A^2} - \nu_A A \qquad \text{(Equation 11)}$$

$$\dot{B} = \left(m(t) + \frac{B^2}{1 + B^2} \right) \frac{1}{1 + A^2/K_A^2} - \nu_B B, \qquad \text{(Equation 12)}$$

where $m(t)$ is the time-dependent input from the morphogen signaling pathway upstream of the GRN. It is a quadratic function of $y(t)$ from Equation 9 or Equation 10 with parameters chosen to place the asymptotic expression domains of A, B in defined locations. Results presented in Figures 4H and 4I and Movie S3 show how this GRN assigns cell fate as a function of time. A detailed description of the hypothesis behind this model is given in Supplemental Experimental Procedures, section 7.

AUTHOR CONTRIBUTIONS

B.S., A.W., A.H.B., and E.D.S. designed the research. B.S., A.W., and E.D.S. performed the research. B.S., A.W., A.H.B., and E.D.S. analyzed the data. B.S., A.W., A.H.B., and E.D.S. wrote the paper.

REFERENCES

Aulehla, A., and Pourquié, O. (2010). Signaling gradients during paraxial mesoderm development. Cold Spring Harb. Perspect. Biol. 2, a000869–a000869.

Balaskas, N., Ribeiro, A., Panovska, J., Dessaud, E., Sasai, N., Page, K.M., Briscoe, J., and Ribes, V. (2012). Gene regulatory logic for reading the Sonic Hedgehog signaling gradient in the vertebrate neural tube. Cell 148, 273–284.

De Angelis, L., Borghi, S., Melchionna, R., Berghella, L., Baccarani-Contri, M., Parise, F., Ferrari, S., and Cossu, G. (1998). Inhibition of myogenesis by transforming growth factor beta is density-dependent and related to the translocation of transcription factor MEF2 to the cytoplasm. Proc. Natl. Acad. Sci. USA 95, 12358–12363.

Dennler, S., Itoh, S., Vivien, D., ten Dijke, P., Huet, S., and Gauthier, J.M. (1998). Direct binding of Smad3 and Smad4 to critical TGF beta-inducible elements in the promoter of human plasminogen activator inhibitor-type 1 gene. EMBO J. 17, 3091–3100.

Gómez-Sjöberg, R., Leyrat, A.A., Pirone, D.M., Chen, C.S., and Quake, S.R. (2007). Versatile, fully automated, microfluidic cell culture system. Anal. Chem. 79, 8557–8563.

Green, J.B., New, H.V., and Smith, J.C. (1992). Responses of embryonic Xenopus cells to activin and FGF are separated by multiple dose thresholds and correspond to distinct axes of the mesoderm. Cell 71, 731–739.

Gurdon, J.B., Standley, H., Dyson, S., Butler, K., Langon, T., Ryan, K., Stennard, F., Shimizu, K., and Zorn, A. (1999). Single cells can sense their position in a morphogen gradient. Development 126, 5309–5317.

Hall, M.P., Unch, J., Binkowski, B.F., Valley, M.P., Butler, B.L., Wood, M.G., Otto, P., Zimmerman, K., Vidugiris, G., Machleidt, T., et al. (2012). Engineered luciferase reporter from a deep sea shrimp utilizing a novel imidazopyrazinone substrate. ACS Chem. Biol. 7, 1848–1857.

Harvey, S.A., and Smith, J.C. (2009). Visualisation and quantification of morphogen gradient formation in the zebrafish. PLoS Biol. 7, e1000101.

Katagiri, T., Yamaguchi, A., Komaki, M., Abe, E., Takahashi, N., Ikeda, T., Rosen, V., Wozney, J.M., Fujisawa-Sehara, A., and Suda, T. (1994). Bone morphogenetic protein-2 converts the differentiation pathway of C2C12 myoblasts into the osteoblast lineage. J. Cell Biol. 127, 1755–1766.

Kerszberg, M., and Wolpert, L. (2007). Specifying positional information in the embryo: looking beyond morphogens. Cell 130, 205–209.

Kutejova, E., Briscoe, J., and Kicheva, A. (2009). Temporal dynamics of patterning by morphogen gradients. Curr. Opin. Genet. Dev. 19, 315–322.

Lee, M.A., Heasman, J., and Whitman, M. (2001). Timing of endogenous activin-like signals and regional specification of the Xenopus embryo. Development 128, 2939–2952.

Liu, D., Black, B.L., and Derynck, R. (2001). TGF-beta inhibits muscle differentiation through functional repression of myogenic transcription factors by Smad3. Genes Dev. 15, 2950–2966.

Massagué, J., Seoane, J., and Wotton, D. (2005). Smad transcription factors. Genes Dev. 19, 2783–2810.

Müller, P., Rogers, K.W., Jordan, B.M., Lee, J.S., Robson, D., Ramanathan, S., and Schier, A.F. (2012). Differential diffusivity of Nodal and Lefty underlies a reaction-diffusion patterning system. Science 336, 721–724.

Saka, Y., and Smith, J.C. (2007). A mechanism for the sharp transition of morphogen gradient interpretation in Xenopus. BMC Dev. Biol. 7, 47.

Schohl, A., and Fagotto, F. (2002). Beta-catenin, MAPK and Smad signaling during early Xenopus development. Development 129, 37–52.

Tapscott, S.J. (2005). The circuitry of a master switch: Myod and the regulation of skeletal muscle gene transcription. Development 132, 2685–2695.

Tu, Y., Shimizu, T.S., and Berg, H.C. (2008). Modeling the chemotactic response of Escherichia coli to time-varying stimuli. Proc. Natl. Acad. Sci. USA 105, 14855–14860.

Warmflash, A., Zhang, Q., Sorre, B., Vonica, A., Siggia, E.D., and Brivanlou, A.H. (2012). Dynamics of TGF-β signaling reveal adaptive and pulsatile behaviors reflected in the nuclear localization of transcription factor Smad4. Proc. Natl. Acad. Sci. USA 109, E1947–E1956.

Wartlick, O., Mumcu, P., Kicheva, A., Bittig, T., Seum, C., Jülicher, F., and González-Gaitán, M. (2011). Dynamics of Dpp signaling and proliferation control. Science 331, 1154–1159.

Wilson, P.A., Lagna, G., Suzuki, A., and Hemmati-Brivanlou, A. (1997). Concentration-dependent patterning of the Xenopus ectoderm by BMP4 and its signal transducer Smad1. Development 124, 3177–3184.

Wolpert, L. (2006). Principles of Development, Third Edition. (Oxford: Oxford University Press).

Zi, Z., Chapnick, D.A., and Liu, X. (2012). Dynamics of TGF-β/Smad signaling. FEBS Lett. 586, 1921–1928.